Comparison between Experimental and SPH Models over a Sharp-crested Weir

M. Lodomez, S. Erpicum, B. Dewals, M. Pirotton and P. Archambeau
University of Liege (ULg), Department ArGEnCo
Hydraulics in Environmental and Civil Engineering
Liege
BELGIUM
E-mail: M.Lodomez@ulg.ac.be

Abstract: *In this paper the numerical simulations of a free surface flow over a sharp-crested weir are presented and compared to experimental results. The numerical model implemented consists of the meshless Smoothed Particle Hydrodynamics (SPH) method which uses Navier-Stokes equations and the Tait equation of state for water. This numerical method has been developed in the framework of a master thesis and aimed to define the characteristics of the free jet. The validation of the results was performed through the analysis of the pressure field and the comparison of the numerical free surface profiles with experimental measurements conducted in the Hydraulic Laboratory of the University of Liège (ULg). A good qualitative agreement has been obtained.*

Keywords: *SPH method, free surface, weir flow.*

1. INTRODUCTION

A key component of dam safety is the spillway whose role is to safely release floods downstream so that the water level in the reservoir does not overtop the dam. The study of the flow over a weir is therefore a fundamental subject of hydraulics. In addition, weirs are hydraulic structures that supply a single relationship between the upstream head and the discharge. This property leads to their wide study and use in many engineering processes such as to regulate the water level of a river, to discharge excess water during floods and to divert water into hydropower plants.
In this paper, the particular case of a sharp-crested weir is considered. According to Bos (1989), weirs are defined as sharp-crested if the upstream head exceeds 15 times the thickness of the weir crest. In our experimental setup, the weir crest consists of a thin plate and its thickness in the streamwise direction is below two millimetres. As a result, the water falls downstream as a free jet. One key interest of the sharp-crested weir is that the trajectory of the jet, particularly the profile of its lower nappe, is used for the design of ogee crested weirs. Indeed, the design conditions of these structures ensure ventilation below the flow by keeping atmospheric pressure on the sides and nappe surfaces.

Traditionally, physical models are built to assess weir operation. Many experimental studies were conducted to reproduce overtopping flows, to calculate discharge coefficient and to fit upper and lower nappe profiles (Bos et al., 1984; Bos, 1989; Sinniger and Hager, 1989; Bagheri and Heidarpour, 2009). Physical models are more time- and cost-demanding than computational models. Besides, numerical models give straightforward access to all hydraulic variables. Nonetheless, despite the rapid evolution of computer modeling to solve the governing equations of hydraulics, a limited number of publications concerning numerical simulations of overtopping flows exist. In Chatila and Tabbara (2004), Gessler (2005), Li et al. (2010) and Savage and Johnson (2001), flows over ogee spillways are numerically modeled using commercial computational fluid dynamics software (Flow-3D, ADINA-F and ANSYS Fluent).
For sharp-crested weirs, two recent works based on the resolution of the two dimensional incompressible Navier-Stokes equations, present numerical results (Qu et al., 2009; Ferrari, 2010) which faithfully reproduce the characteristics of flow over sharp-crested weirs. Qu et al. (2009) solve the governing equations using the volume of fluid (VOF) method while Ferrari (2010) uses the Smoothed Particle Hydrodynamic (SPH) method which is an interesting alternative to mesh-based approaches. As exposed in Saunders et al. (2014), the benefits of SPH for spillway modelling, compared to mesh-based methods, include an automatic representation of free surface flow behavior due to the Lagrangian nature of the model and the intrinsic ability to consider complex geometries. The major drawback of this method is the longer computation time. However, the advantages of the

method in the near future could outweigh its disadvantages. In this context, a master's thesis was undertaken at ULg to develop a 2D SPH model and simulate free jet (Lodomez, 2014). This paper sums up the results of this work and, particularly, the results of a flow over sharp-crested weir simulations and their comparisons with experimental results.

2. EXPERIMENTAL MODEL

2.1. Experimental setup and procedure

To determine the profile of the jet, an experimental model of a sharp-crested weir was built in the hydraulic laboratory of the University of Liege (Lodomez, 2014). The model is composed of a reservoir width of 0.9 m, a weir height of 2.8 m and a channel width of 0.2 m (Figure 1(b-c)). Walls in polyvinyl chloride (PVC) were added in the reservoir for reducing the flow section to the width of the spillway (0.20 m). The flow was thus confined in a 2D-vertical slice passing by the centreline of the spillway and contraction effects affecting the nappe stability were therefore minimized (Vermeyen, 1992). The downstream edge of the PVC weir crest was bevelled as shown in Figure 1(a) and ventilated through a metal pipe which stiffens this weir crest. The upstream head, h, was measured 1.5 m upstream of the weir crest using a point gauge with accuracy of the order of 1mm. At this location, the kinetic energy is negligible and h is therefore the total head. Seven discharges were tested: from 56 l/s to 156 l/s. The discharge over the weir was measured upstream of the reservoir using an electromagnetic flow meter with an accuracy of ± 0.5 %. The nappe profiles were determined manually using a reference grid on the sidewall.

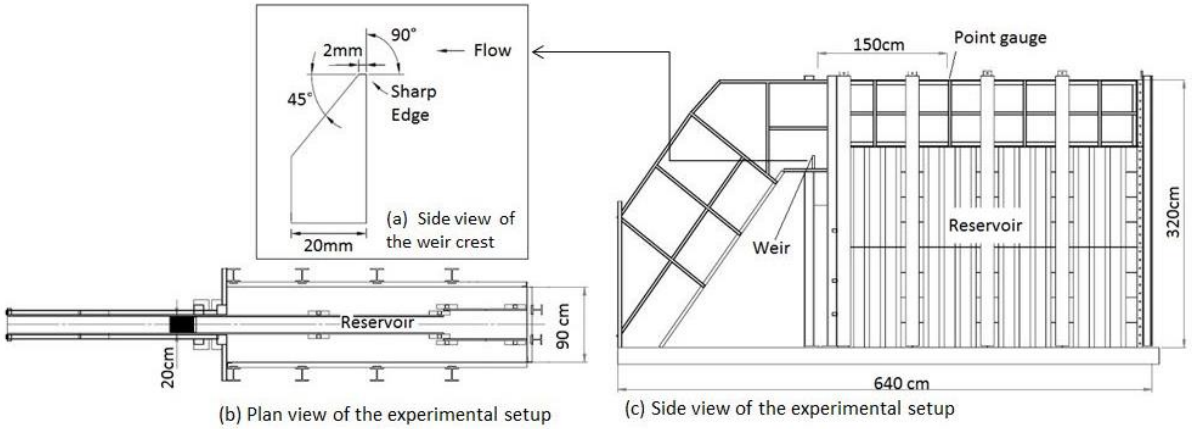

Figure 1 - Weir setup

2.2. Results

The measured upper and lower profiles of the jet over the sharp-crested weir are plotted in dimensionless form in Figure 2. These experimental results were obtained by dividing the coordinates (i.e. x, the distance downstream of the weir and y, the vertical elevation) of each measured point by the upstream head, h. Using a least square approach, the upper and lower nappe profiles were approximated by, respectively, a polynomial of order 3 and 4 (Eq. [2] and[1]). The coefficients of determination R^2 of these formulations are equal to 0.9996 and 0.9978 respectively for the upper and lower nappe profiles. Moreover, Lodomez (2014) showed that this experimental formulation is consistent with formulations given in literature, such as the Hager and Bagheri formulations (Sinniger and Hager, 1989; Bagheri and Heidarpour, 2009).

$$\frac{y}{h} = -0.0455\left(\frac{x}{h}\right)^3 - 0.2269\left(\frac{x}{h}\right)^2 - 0.2217\left(\frac{x}{h}\right) + 0.8729 \qquad for -1 < \left(\frac{x}{h}\right) < 2 \qquad [1]$$

$$\frac{y}{h} = -0.2871\left(\frac{x}{h}\right)^4 + 1.1018\left(\frac{x}{h}\right)^3 - 1.9044\left(\frac{x}{h}\right)^2 + 0.8773\left(\frac{x}{h}\right) + 0.0217 \qquad for\ 0 < \left(\frac{x}{h}\right) < 1.5 \qquad [2]$$

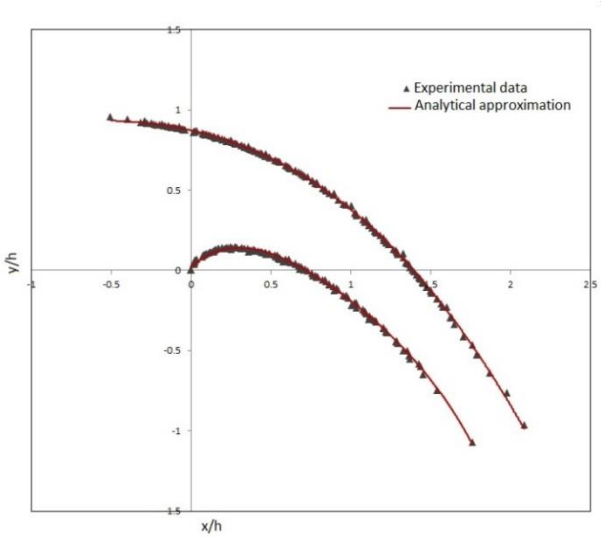

Figure 2 - Upper and lower nappe profiles over a sharp-crested weir

3. NUMERICAL MODEL

3.1. Governing equations

The mathematical model used to simulate the flow over sharp-crested weirs consists in the Navier-Stokes equations for weakly compressible isothermal flows. The system of governing partial differential equations is given by:

$$\frac{d\rho}{dt} = -\rho\vec{\nabla}\cdot\vec{v} \qquad [3]$$

$$\frac{d\vec{v}}{dt} = \frac{1}{\rho}\vec{\nabla}\underline{\underline{\sigma}} + \vec{S} \qquad [4]$$

$$\frac{d\vec{x}}{dt} = \vec{v} \qquad [5]$$

Equations [3] and [4] express the mass and momentum balance in a non-conservative form. Equation [5] updates the position of each infinitesimal fluid element of the continuum. The term $\frac{d}{dt}$ represents the total derivative and the variables present in these equations are the density ρ, the velocity $\vec{v}$ and the position $\vec{x}$. The vector $\vec{S}$ represents the body forces per unit of mass and the total stress tensor $\underline{\underline{\sigma}}$ is defined as:

$$\underline{\underline{\sigma}} = -p\underline{\underline{I}} + \underline{\underline{\tau}}, \qquad [6]$$

where p is the pressure, $\underline{\underline{I}}$ the unit tensor and $\underline{\underline{\tau}}$ the viscous stress tensor.

In line with the standard SPH approach, Tait equation has been used to close the system by relating pressure to density:

$$p = B\left(\left(\frac{\rho}{\rho_0}\right)^{\gamma} - 1\right) \qquad [7]$$

$$B = \frac{c_0^2\rho_0}{\gamma} \qquad [8]$$

with ρ_0 the reference fluid density at atmospheric pressure and γ a constant usually taken equal to $\gamma = 7$. The coefficient B given by Eq. [8] depends on the speed of sound and is adapted to keep density fluctuations negligible (Monaghan and Kos, 1999).

3.2. The SPH formulation

Smoothed Particle Hydrodynamics (SPH) is a meshless Lagrangian method introduced by Gingold and Monaghan (1977) and Lucy (1977) to solve astrophysical problems. SPH was later adapted to simulate free surface flows (Monaghan, 1994). Thanks to its adaptive character and its meshless features, SPH applies now to simulate a broad spectrum of flow patterns (Liu and Liu, 2003).
According to the SPH approach, the fluid continuum is discretized as a finite set of arbitrarily distributed particles, characterized by their physical properties such as density ρ, pressure p, velocity $\vec{v}$ and position $\vec{x}$. These particles move in space and time and interact with each other within a given influence distance. This influence range is assigned to the particles by means of a smoothing function, also called kernel and used to smooth the discrete information stored by each particle.
The governing equations introduced previously (Eqs [3]-[5]) can be rewritten in SPH formalism (Liu and Liu, 2003). For each particle, this involves to the replacement of the partial differential equations in integral form by summations over the particles in a local neighbourhood. The governing equations in the SPH formalism for the i^{th} particle write as follows, as a function of the neighbouring particles j:

$$\frac{d\rho_i}{dt} = \sum_{j=1}^{N} m_j \vec{v}_{ij} \cdot \overrightarrow{\nabla_i} W_{ij} \qquad [9]$$

$$\frac{d\vec{v}_i}{dt} = -\sum_{j=1}^{N} m_j \left(\frac{p_i}{\rho_i^2} + \frac{p_j}{\rho_j^2} + \Pi_{ij} \right) \cdot \overrightarrow{\nabla_i} W_{ij} + \overrightarrow{S_{ij}} \qquad [10]$$

$$\frac{d\overrightarrow{x_i}}{dt} = \overrightarrow{v_i} \qquad [11]$$

where $\vec{v}_{ij} = \vec{v}_i - \vec{v}_j$, Π_{ij} is the artificial viscosity and $\overrightarrow{\nabla_i} W_{ij}$ the gradient of the smoothing function centered at the particle i. The kernel function W_{ij}, which assigns to neighbouring particles a weight depending on their distance to particle i, is a cubic B-spline (Monaghan and Lattanzio, 1985):

$$W_{ij} = \alpha_d \begin{cases} \frac{2}{3} - \left(\frac{r_{ij}}{h_{ij}}\right)^2 + \frac{1}{2}\left(\frac{r_{ij}}{h_{ij}}\right)^3 & if \quad 0 \le \left(\frac{r_{ij}}{h_{ij}}\right) < 1 \\ \frac{\left(2 - \frac{r_{ij}}{h_{ij}}\right)^3}{6} & if \quad 1 \le \left(\frac{r_{ij}}{h_{ij}}\right) \le 2 \\ 0 & if \quad \left(\frac{r_{ij}}{h_{ij}}\right) > 2 \end{cases} \qquad [12]$$

- $\vec{r}_{ij} = \vec{x}_i - \vec{x}_j$ is the distance between the particles i and j.
- α_d is a coefficient used to normalize the kernel $(\int W\, dV = 1)$. In 2D, its value is given by $\alpha_d = 15/(7\pi h_{ij}^2)$.
- h_{ij} is the smoothing length. In the framework of this paper the smoothing length is assumed constant in space but variable in time (Goffin, 2013; Lodomez, 2014), as suggested in Monaghan and Lattanzio (1985).

The term Π_{ij} represents a repulsive force acting between particles when they are close to each other:

$$\Pi_{ij} = \begin{cases} \mu_{ij} \dfrac{-\alpha \overline{c_{ij}} + \beta \mu_{ij}}{\overline{\rho_{ij}}} & if \quad \overrightarrow{v_{ij}} \cdot \overrightarrow{r_{ij}} < 0 \\ 0 & if \quad \overrightarrow{v_{ij}} \cdot \overrightarrow{r_{ij}} \ge 0 \end{cases} \qquad [13]$$

α and β are two viscosity parameters, $\bar{c}_{ij}$ and $\bar{\rho}_{ij}$ are the mean celerity and density of the fluid between particles i and j, and the term μ_{ij} is defined by Monaghan (1992) as:

$$\mu_{ij} = h_{ij} \frac{\vec{v}_{ij} \cdot \vec{r}_{ij}}{r_{ij}^2 + \eta^2} \qquad \text{with} \qquad \eta^2 = 0.01 h_{ij}^2 \ . \qquad [14]$$

Although this approach lacks physical meaning and requires a careful calibration of the parameters, it is easy to implement and was therefore adopted. More physical formulations exist, as outlined in Dalrymple and Rogers (2006).

The SPH formulation [9]-[11] was integrated over time using an explicit Runge-Kutta scheme. The time step was constrained by the Courant condition, body force and viscous diffusion terms as introduced in Monaghan (1992).

3.3. Application to the flow over a sharp-crested weir

The considered geometry consists of a 5 m long reservoir and a 2.8 m high sharp-crested weir. As depicted in Figure 3, two types of particles are used:

- mobile particles in the fluid domain,
- fixed particles simulate the solid boundaries of the domain such as the bottom, the walls and the weir; …

Solid particles are implemented by prescribing stringent constraints on their motion, thanks to the repulsive forces reproduced in the model.

Three types of boundaries are considered (Figure 3):

- on the left, the open boundary corresponds to the inflow of particles, which are injected with a prescribed velocity;
- on the right, the open boundary is an outflow where particle are removed from the computational domain;
- the moving interface corresponding to the free surface evolves freely in space and over time.

The water depth prescribed initially z is chosen slightly higher than the weir height h_w. The fluid domain is discretized in average by 175,000 SPH particles with an initial particle spacing of 0.01 m. The computational time is of the order of 24 hours on a 3.33GHz 6-core processor, and is highly influenced by the number of particle.

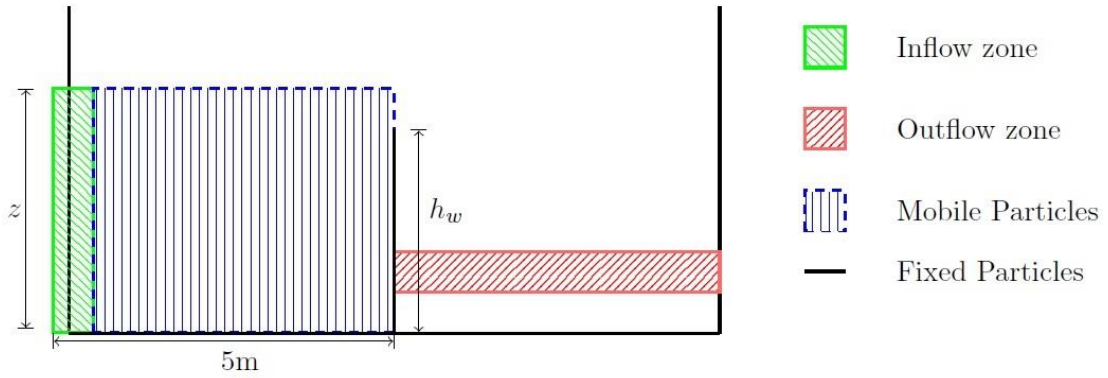

Figure 3 - Initial condition used for the SPH simulation of the flow over a sharp-crested weir.

In Figure 4, the evolution of the pressure distribution is plotted for a discharge of 156 l/s. The flow is mostly established after 10 seconds. The profile remains mainly hydrostatic in the reservoir; but slight pressure disturbances are observed close to the upstream boundary, as a result of the inflow of new particles. The obtained velocity field is in qualitative agreement with the observations (Figure 5).

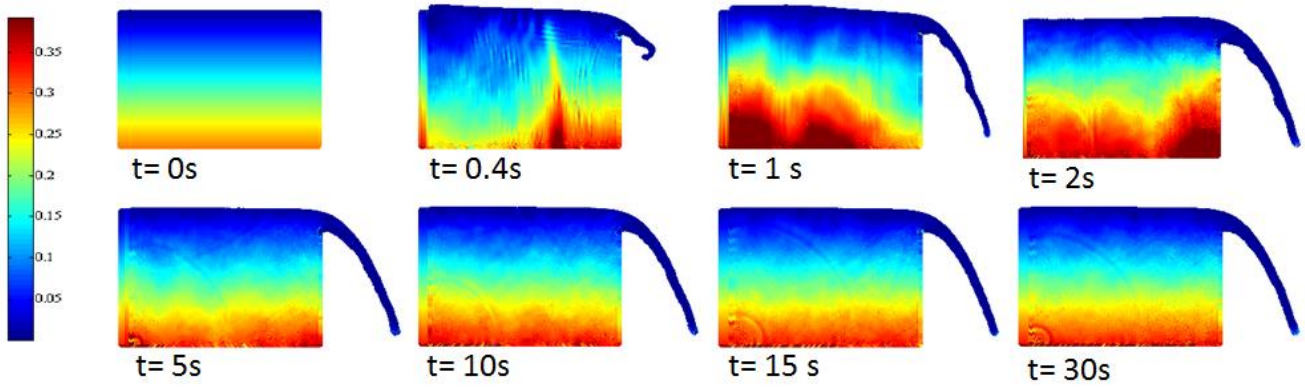

Figure 4 - Time evolution of the pressure distribution [bar].

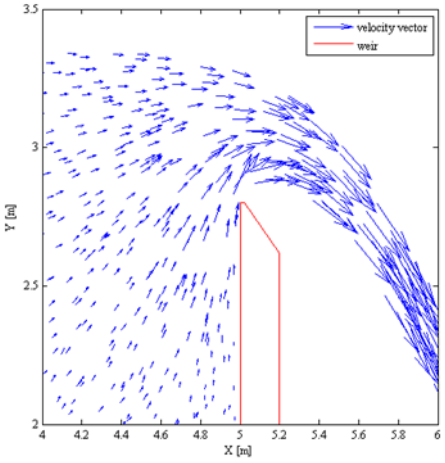

Figure 5 - Velocity field.

4. COMPARISON BETWEEN OBSERVED AND COMPUTED RESULTS

The numerical results presented in section 3.3 are compared to the experimental measurements discussed in section 2. Figure 6 and Figure 7 show in dimensionless form the envelope of particles trajectories in the simulations and the location of the lower and upper nappe profiles as observed experimentally [Eqs (1)-(2)].

Figure 7 reveals a good overall agreement between the SPH results and the experiments; except for the lower nappe profile immediately downstream of the weir crest. In addition, the jet is globally drawn in toward the air pocket. Indeed, for x/d higher than 0.7, some particles are located below the experimental curves. These two observations can be linked to the type of fixed boundary particles implemented in this code and an associated excessive repulsive force that modifies the velocity field and therefore the curvature of the jet. These observations are confirmed in Figure 6, which shows the envelope of the particles trajectories between 10 to 30 seconds.

The upstream head was measured experimentally and is equal to 0.565 m for a discharge of 156 l/s. The numerical model predicts a value of 0.562 m, which is a very good match considering the initial spacing of 0.01 m between the particles. Hence, the model succeeds in representing the free surface flow in the reservoir and depicts qualitatively the jet over the sharp-crested weir.

The simulations were repeated for different discharges and different initial water depth z, as shown in Table 1. The weir height remained equal to the experimental one, i.e. 2.8 m.

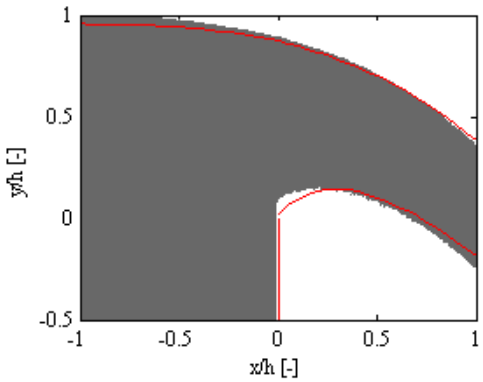

Figure 6 - Comparison between the numerical free surface profiles and the experimental relations in red. The numerical results refer to the superposition of all particles between 10 and 30 s.

Simulations	Discharge *[l/s]*	*z [m]*
A_1		3.3
A_2	156	3
A_3		2.8
B_1	89	2.8
B_2	111	3

Table 1 - Set of simulations to test the influence of the main parameters

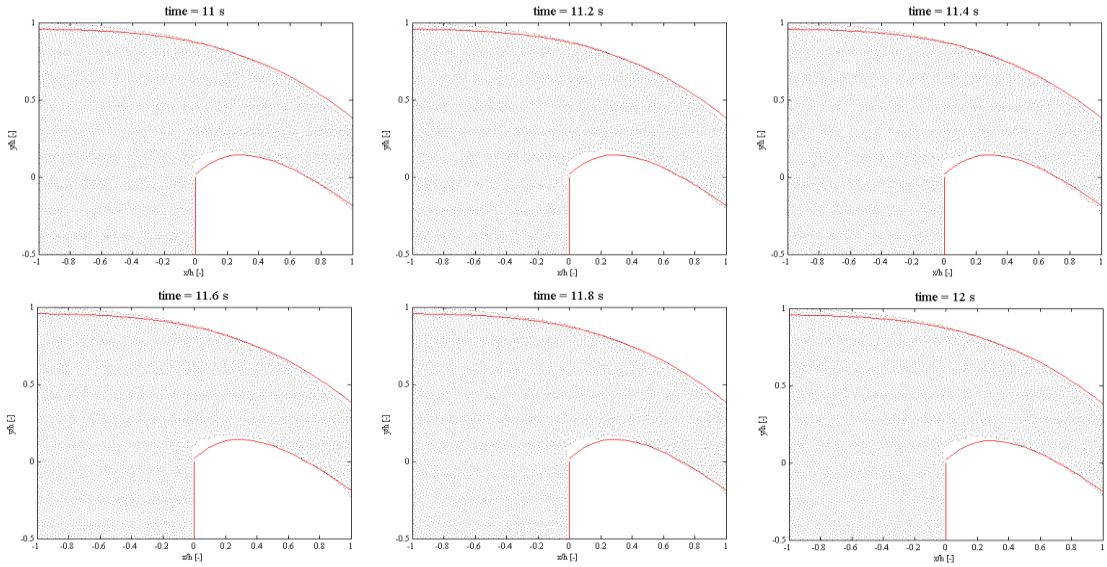

Figure 7 - Envelope of computed flow trajectories (grey area)
and experimental relations Eqs (1)-(2) (red).

Comparing simulations A_1, A_2 and A_3 demonstrates that the initial water level has no significant influence on the final results. Indeed, the upstream head for these three simulations is respectively 0.562 m, 0.559 m and 0.554 m. The measured upstream head being equal to 0.565m, the relative error remains below 2 %.

As shown in Figure 8 and Table 2, the conclusions drawn from the numerical model for the discharge of 156 l/s may be transposed to other discharges. Indeed, for simulations B_1 and B_2, the calculated upstream heads are also close to the experimental ones. Moreover the global behavior of the flows depicted in Figure 8 is similar to the behavior obtained for a discharge of 156 l/s.

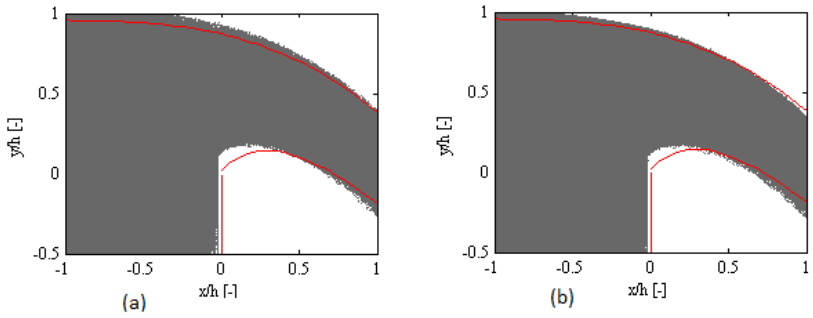

Figure 8 - Comparison between the numerical free surface profiles and the experimental relations (Eqs 13-14) in red for simulation (a) B_1 and (b) B_2.

Simulations	Experimental [m]	Numerical [m]	Relative error [%]
B_1	0.406	0.391	3.7
B_2	0.474	0.451	4.8

Table 2 - Measured vs. computed upstream heads

5. CONCLUSION

There is a pressing engineering need for improved computational models for flow over spillways and, particularly, sharp-crested weirs. The flow complexity makes it challenging from the numerical perspective. In this context, the jet flow over a sharp-crested weir has been simulated by a self-developed Smoothed Particle Hydrodynamic (SPH) model. This method solves the weakly compressible Navier-Stokes equations coupled with the Tait equation of state. It is very adapted to the considered type of problem. A satisfactory agreement was obtained between numerical results and experimental observations. Improvements are still needed regarding (i) the numerical treatment of fixed boundaries and (ii) the artificial viscosity term. Although more complex, implementing real laminar or turbulent viscosity seems essential to achieve a fully realistic flow representation.

6. REFERENCES

Bagheri, S., Heidarpour, M., 2009. Flow over rectangular sharp-crested weirs. Irrigation Science 28, 173–179.

Bos, M.G., 1989. Discharge measurement structures. Discharge measurement structures.

Bos, M.G., Replogle, J.A., Clemmens, A.J., 1984. Flow measuring flumes for open channel systems.

Chatila, J., Tabbara, M., 2004. Computational modeling of flow over an ogee spillway. Computers and Structures 82, 1805–1812.

Dalrymple, R.A., Rogers, B.D., 2006. Numerical modeling of water waves with the SPH method. Coastal Engineering 53, 141–147.

Ferrari, A., 2010. SPH simulation of free surface flow over a sharp-crested weir. Advances in Water Resources 33, 270–276.

Gessler, D., 2005. CFD modeling of spillway performance, in: WorldWaterCongress2005Impacts Global Climate Change - Proceedings2005WorldWater Environmental Resources Congress. p. 398.

Gingold, R.A., Monaghan, J.J., 1977. Smoothed particle hydrodynamics: theory and application to non-spherical stars. Monthly notices of the royal astronomical society 181, 375–389.

Goffin, L., 2013. Development of a didactic SPH model.

Li, S., Cain, S., Wosnik, M., Miller, C., Kocahan, H., Wyckoff, R., 2010. Numerical modeling of probable maximum flood flowing through a system of spillways. Journal of Hydraulic Engineering 137, 66–74.

Liu, G.-R., Liu, M.B., 2003. Smoothed particle hydrodynamics: a meshfree particle method. World Scientific.

Lodomez, M., 2014. Determining the characteristics of a free jet in 2-D by the SPH model.

Lucy, L.B., 1977. A numerical approach to the testing of the fission hypothesis. The astronomical journal 82, 1013–1024.
Monaghan, J., Kos, A., 1999. Solitary Waves on a Cretan Beach. Journal of Waterway, Port, Coastal, and Ocean Engineering 125, 145–155.
Monaghan, J.J., 1992. Smoothed particle hydrodynamics. Annual Review of Astronomy and Astrophysics 30, 543–574.
Monaghan, J.J., 1994. Simulating Free Surface Flows with {SPH}. Journal of Computational Physics 110, 399–406.
Monaghan, J.J., Lattanzio, J.C., 1985. A refined particle method for astrophysical problems. Astronomy and astrophysics 149, 135–143.
Qu, J., Ramamurthy, A.S., Tadayon, R., Chen, Z., 2009. Numerical simulation of sharp-crested weir flows. Canadian Journal of Civil Engineering 36, 1530–1534.
Saunders, K., Prakash, M., Cleary, P.W., Cordell, M., 2014. Application of Smoothed Particle Hydrodynamics for modelling gated spillway flows. Applied Mathematical Modelling 38, 4308–4322.
Savage, B.M., Johnson, M.C., 2001. Flow over ogee spillway: Physical and numerical model case study. Journal of Hydraulic Engineering 127, 640–648.
Sinniger, R., Hager, W., 1989. Constructions Hydrauliques : écoulemetns stationnaires.
Vermeyen, T.B., 1992. Uncontrolled Ogee Crest Research.